



ELSEVIER

Journal of Photochemistry and Photobiology A: Chemistry 124 (1999) 67–73

Journal of  
Photochemistry  
and  
Photobiology  
A: Chemistry

## Excited states properties of some phenoxathiin derivatives

Sorana Ionescu<sup>a</sup>, Daniela Gavriliu<sup>b</sup>, Ovidiu Maior<sup>b</sup>, Mihaela Hillebrand<sup>c,\*</sup>

<sup>a</sup>National Institute for Development of Chemical Pharmaceutical Research, Sos. Vitan, Bucharest, Romania

<sup>b</sup>Department of Organic Chemistry, Faculty of Chemistry, University of Bucharest, Sos. Panduri, Bucharest, Romania

<sup>c</sup>Department of Physical Chemistry, Faculty of Chemistry, University of Bucharest, Bd. Elisabeta, Nr. 4-12, Bucharest, Romania

Received 11 January 1999; received in revised form 2 March 1999; accepted 5 March 1999

### Abstract

Several properties of the excited singlet state (natural lifetimes, fluorescence quantum yields, solvatochromicity, etc.) of some 3-substituted phenoxathiin derivatives (methyl, formyl, acetyl) were investigated by means of absorption and steady-state fluorescence spectroscopy. The results point out that the emission properties are dependent on the type of the substituent, the most efficient being 3-acetylphenoxathiin. The effect of the solvent polarity on the fluorescence maxima of 3-formyl- and 3-acetylphenoxathiin, rationalized in terms of the Lippert–Mataga equation, points at an increase in the dipole moment in the excited state. A specific behavior in protic solvents was also noticed. AM1 calculations for the ground and excited states support the experimental data and explain the higher efficiency of the carbonyl containing derivatives in terms of a different nature of the first excited singlet. It was established that the enhanced radiative decay for these compounds is due to the presence of new low-lying vacant  $\pi$ -molecular orbital situated between the frontier orbitals of phenoxathiin. The theoretical results reflect also the charge transfer character of the excited states in agreement with the solvatochromicity already discussed. © 1999 Elsevier Science S.A. All rights reserved.

**Keywords:** Phenoxathiin; Steady-state fluorescence; Absorption spectroscopy; AM1 calculations; Excited-state properties

### 1. Introduction

The larger sensitivity of the spectrofluorimetric methods as against the spectrophotometric ones determines an increase in the interest of using fluorophores in the biochemical studies at the molecular level. For the synthesis of such fluorescent probes some bicyclic and tricyclic heteroaromatic systems were used so far.

The sulfur-containing anthracene-like heterocycles, phenoxathiin, phenothiazine, are characterized by weak fluorescent properties, while at low-temperature significant phosphorescent quantum yields have been reported [1,2]. In the study of the photochemistry and photophysics of aromatic sulfoxides at 77 K, Jenks et al. [2] evidenced the triplet state of phenoxathiin ( $23\,783\text{ cm}^{-1}$ ) and reported the value of the phosphorescence quantum yield,  $\Phi_{\text{ph}} = 0.84$ . These properties are correlated with an enhanced probability of intersystem crossing deactivation pathways due to the presence of the sulfur atom. However, some phenothiazine derivatives, substituted either at the nitrogen atom in the central ring or at the position 2 of

the heterocycle [3,4] present good enough fluorescent properties to be used for analytical purposes and structural correlations. During the study of the electronic properties and reactivity in the phenoxathiin class we found that, in spite of the emission properties of the parent heterocycle, some phenoxathiin derivatives also present fluorescent properties.

It is the aim of this paper to outline, by both experimental and theoretical methods, the effect on the emission properties of the substitution in the position 3 of phenoxathiin.

The structures of the investigated compounds are presented in Fig. 1.

### 2. Experimental and theoretical methods

The absorption spectra and the steady-state fluorescence spectra were recorded with a UNICAMM–Helios  $\alpha$  spectrophotometer, and, respectively, with an AMINCO–BOWMAN spectrofluorimeter, using solvents with different polarities. The solvents were Aldrich and Fluka, spectroscopic grade, and were checked for fluorescence and used without further purification. Phenox-

\*Corresponding author. E-mail: mihh@math.math.unibuc.ro

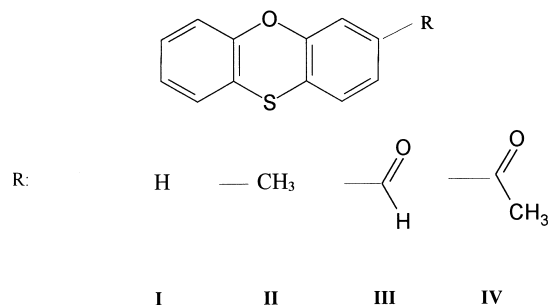


Fig. 1. Formula of the investigated compounds.

athiin derivatives were synthesized as previously described [5].

The radiative lifetimes were estimated by the formula of Strickler and Berg [6]:

$$\frac{1}{\tau_0} = 2.88 \frac{g_1 n_f^3}{g_2 n_a} \frac{\int F(\nu) d\nu}{\int F(\nu) \nu^{-3} d\nu} \int \frac{\varepsilon(\nu)}{\nu} d\nu$$

where  $g_1$ ,  $g_2$  are the multiplicities of the ground and excited states, respectively,  $n_a$ ,  $n_f$  the refractive indexes of the solvent at the longwave of the absorption and fluorescence maxima, respectively; in our case, we considered  $n_f = n_a$ ;  $F(\nu)$  and  $\varepsilon(\nu)$  the intensities of the emission and molar absorption coefficients.

In order to evaluate  $\int (\varepsilon(\nu)/\nu) d\nu$ , a deconvolution of the spectra was previously performed in cases of partially overlapping bands. The estimated errors were ca. 8–9%.

The fluorescence quantum yields,  $\Phi_f$ , were determined relative to quinine sulfate in 1N H<sub>2</sub>SO<sub>4</sub>,  $\Phi_f = 0.55$ , using the same excitation wavelength,  $\lambda = 360$  nm for the reference and the sample; the absorbances of the solutions were lower than 0.08.

The theoretical calculations were performed using the PC version of P. Burk and I. Koppel (public domain) of the MOPAC-7 method. The AMI hamiltonian and EF optimization procedure were used for the ground and the first excited singlet and triplet states. Several levels of configurational interaction were implied using the key words OPEN(n1,n2) and C.I.(n,m). For the formyl and acetyl derivatives, the optimization was done considering both conformers generated by the in-plane position of the carbonyl group, hereafter labeled as **IIIa**, **IIIb** and, respectively, **IVa**, **IVb**.

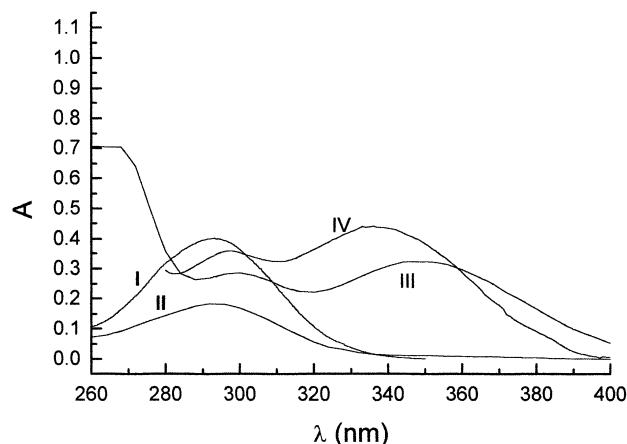


Fig. 2. Electronic absorption spectra in methanol in the 280–350 nm range.

### 3. Results and discussion

#### 3.1. Electronic spectra

Two overlapping bands at 238 and 241 nm and a lower intensity one at 292 nm characterize the electronic spectrum of phenoxathiin, **I**, (Fig. 2). This band, assigned to the  $m \rightarrow m + 1$  transition [7,8], corresponds to the first excited singlet ( $S_1$ ) implied in the emission properties and mainly deactivated by nonradiative processes.

Considering the changes brought about by the substituents in this spectral region, the following observations can be made (Table 1):

- The spectrum of the 3-methyl substituted derivative, **II**, is very similar to that of phenoxathiin, attesting that the methyl group does not, to a great extent, perturb the electronic structure of the heteroaromatic ring. Hence, no real changes in the emission properties are expected.
- In the spectra of the other two derivatives, **III** and **IV**, besides the shift of the phenoxathiin band from 292 toward 300 nm, a new band located at longer wavelengths, namely 338–350 nm is present. For both the compounds, the position of this new band is slightly influenced by the polarity of the solvents, only a small bathochromic shift being noted in the cyclohexane–methanol range.

Table 1  
Spectral features ( $\lambda$  nm,  $\varepsilon$  cm<sup>-1</sup> M<sup>-1</sup>) of the investigated compounds in the 290–350 nm range

Compound	Cyclohexane				Methanol			
	$\lambda$	$\varepsilon$	$\lambda$	$\varepsilon$	$\lambda$	$\varepsilon$	$\lambda$	$\varepsilon$
<b>I</b>	294	4520	—	—	294	3471	—	—
<b>II</b>	294	4588	—	—	294	3500	—	—
<b>III</b>	299	4024	347	5800	300	4160	349	4729
<b>IV</b>	298	3660	337	4437	300	4192	343	5196

Table 2  
Fluorescence maxima,  $\lambda_f$ (nm) in cyclohexane and methanol

Compound	Cyclohexane	Methanol
<b>I</b>	370	381
<b>II</b>	377	402
<b>III</b>	422	529
<b>IV</b>	416	516

– The ratio of the intensity of these two bands,  $\varepsilon_{350}/\varepsilon_{300}$  for solvents ranging from nonpolar (cyclohexane, heptane) to protic polar ( $\text{CH}_3\text{OH}$ ) is in the 1.26–1.17 range for **III** and more dependent on the solvent polarity, 1.44 vs. 1.10 for **IV**.

These aspects point out that a different excited state will be implied in the fluorescence spectra of **III** and **IV** relative to **I** and **II**. As both, **III** and **IV** are carbonyl-containing compounds this first excited singlet could be either of the  $\pi-\pi^*$  or  $n-\pi^*$  type. On experimental grounds, i.e., molar absorptivities, bathochromic shifts in polar solvents we assign these bands to  $\pi-\pi^*$  transitions.

### 3.2. Fluorescence spectra

The emission wavelengths in cyclohexane and methanol are listed in Table 2.

Although there is a bathochromic shift from cyclohexane to methyl alcohol for all the compounds, for **III** and **IV** this shift is very large and prompted us to undertake a systematic study of the dependence of emission properties on the solvent polarity.

The results obtained using nonpolar, polar aprotic and protic solvents are presented<sup>1</sup> as plots of the fluorescence maxima against the solvent polarity function

$$v_f = v_{f_0} - \frac{2(\Delta\mu)^2}{hc\rho^3} F(\varepsilon, n) \quad F(\varepsilon, n) = \frac{\varepsilon - 1}{2\varepsilon + 1} - \frac{n^2 - 1}{2(n^2 + 1)}$$

$v_f$  vs.  $F(\varepsilon, n)$  [9], in which  $\Delta\mu$  represents the increase in the dipole moment value in the excited state and  $\rho$  the radius of the solvent cavity.

The plots (Fig. 3) indicate that the experimental data do not follow the linear relationship of Lippert–Mataga over the whole solvent polarity range.

The slopes of the linear segment of the plots were used for estimating the increase of the dipole moment values in the excited state ( $\Delta\mu$ ). It can be seen, (Table 3) that considering the radius of the cavity within the limits 3.0–3.5 Å (ca. 40% of the longest diameter) [10] the increase in the dipole moments is significant, especially for **III**. The quantum yields of **II** and **III** (Table 4) are also influenced by the solvent polarity: there is an increase from nonpolar to

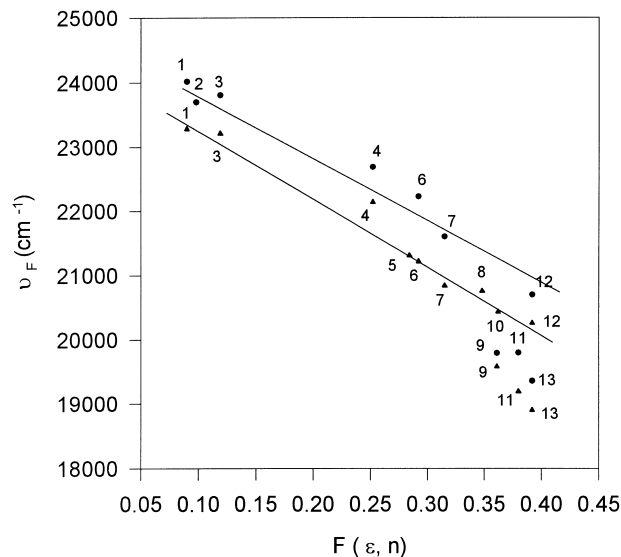


Fig. 3. Dependence of the fluorescence maxima,  $v_f$  on the solvent polarity function,  $F(\varepsilon, n)$ .

moderately polar solvents, followed by a decrease in protic solvents.

Strong deviations from the Lippert–Mataga linearity in polar or protic solvents and the quantum-yield dependence of the solvent polarity are mentioned in literature [11–14] and explained either by some specific interactions (in protic solvents mainly by hydrogen bonds) or by deactivation channels due to the presence of TICT states. In our case, we consider as more probable the interactions by hydrogen bonds and experiments on the inclusion complexes in the hydrophobic cavity of  $\beta$ -cyclodextrines are in progress to support this explanation.

The fluorescence quantum yields and the radiative lifetimes measured using the Strikler and Berg [6] formula allows for an estimation of the lifetime of the excited state in methanol for **III** and **IV** (Table 5). In order to test at least the order of magnitude for these values, quenching experiments were performed in the presence of potassium iodide considering that the iodine ion is a representative quencher for diffusion-controlled processes. Under the assumption that  $k_{\text{obs}} = k_{\text{diff}}$ , the Stern–Volmer quenching constants,  $K_{\text{SV}}$  were used to obtain values for  $\tau_f$ ,  $k_f$  and  $k_{\text{nrad}}$ . The results listed in Table 5 show that the agreement is good for **IV** and acceptable for **III**; the lifetime of the excited state of these

Table 3  
Experimental estimation of the increase in the dipole moment values in the excited state

Compound	Correlation coefficient	$\rho$ (Å)	$\Delta\mu$ (D)
<b>III</b>	0.94	3.5	7.0
		3.0	5.5
<b>IV</b>	0.98	3.5	8.0
		3.0	6.3

<sup>1</sup>As the absorption spectra are practically not influenced by the solvent polarity, the dependence of the Stokes shift on the solvent polarity function was not considered.

Table 4  
Influence of the solvent polarity on the fluorescence quantum yields

Compound	Cyclohexane	Ethyl ether	Ethyl acetate	DCM	Ethanol	Methanol
<b>III</b>	0.01	0.09	0.24	0.45	0.12	0.11
<b>IV</b>	0.01	0.07	0.20	0.52	0.25	0.19

carbonyl-containing derivatives is of the order of 2–5 ns and the constant rates for nonradiative processes are significant.

### 3.3. MO calculations

The MO calculations were performed in order to get a deeper insight on the electronic structure of the compounds and to account for some of the experimental data. We attempted to explain the differences between **I** and **II**, on the one hand, and the formyl and acetyl derivatives, on the other, and the significant solvatochromic effect for these latter.

The AM1 optimized ground-state geometries of the investigated compounds present folded shapes with a dihedral angle of ca. 165°, similar to that found by Amato et al. [15] for phenoxathiin, using the PM3 hamiltonian. A better understanding of the features of the molecular orbitals and, consequently, of the nature of the electronic transitions can be obtained on looking at the results obtained by means of a simplified model. We will consider that in the anthracene-like heterocycles the MOs result from the interaction of the  $\pi$  molecular orbitals of the two phenyl rings through the heteroatomic bridge.

In the case of phenoxathiin, the MO will be given by the expression:

$$\varphi = c_{iA}\phi_{iA} + c_{iB}\phi_{iB} + c_S\chi_S + c_O\chi_O,$$

where  $\phi_{iA}$ ,  $\phi_{iB}$  represent the  $\pi$  molecular orbitals of the two benzene rings (A, B) and  $\chi_S$ ,  $\chi_O$  the atomic  $p_z$  orbitals of sulfur and oxygen.

The last occupied MOs will be determined by the interaction of the degenerate benzene orbitals,  $\phi_{2A}$ ,  $\phi_{3A}$ , respectively,  $\phi_{2B}$ ,  $\phi_{3B}$  ( $\varepsilon = -9.65$  eV) with the atomic  $\chi_S$ ,  $\chi_O$  orbitals. The system presents  $C_s$  symmetry, and the molecular orbitals can be classified as symmetric (sym) or antisymmetric (asym) in respect to a plane passing through

the heteroatoms. From the MOs of the benzenic rings, the following two combinations can be built:

$$\phi_i^{\text{Sym}} = 1/\sqrt{2}(\phi_{iA} + \phi_{iB})$$

$$\phi_i^{\text{Asym}} = 1/\sqrt{2}(\phi_{iA} - \phi_{iB})$$

The symmetric orbitals are the only ones which can further interact with  $\chi_S$ ,  $\chi_O$ ; the asymmetric ones, having no contribution from the heteroatoms, will maintain energies close to that in the isolated benzene. The symmetric interaction ( $\phi_2^{\text{Sym}}$ ,  $\phi_3^{\text{Sym}}$ ,  $\chi_S$ ,  $\chi_O$ ) lead to four occupied molecular orbitals extended over the whole molecule as the oxygen  $2p_z$  orbital is lower in energy than the degenerate benzenic orbitals ( $-13.52$  eV vs.  $-9.65$  eV) its contribution in the last occupied MOs of phenoxathiin will be insignificant. Therefore, in the range of the last occupied molecular orbitals we expect the two antisymmetric MO localized only on the benzenic rings and the three symmetric orbitals localized on the sulfur as well as on the benzenic rings. As the sulfur atomic orbital has the highest energy in this series, ( $\varepsilon_s = -7.25$  eV), its contribution will be enhanced in homo. The same procedure applied to the vacant MOs point out that, in phenoxathiin, the lowest empty orbitals will correspond to the interaction of the benzenic  $\phi_4$ ,  $\phi_5$  orbitals. The AM1 molecular orbital energies are listed in Table 6 and the contours of some orbitals are presented in Fig. 4.

It can be seen that the calculated results, the energies and the shapes of the symmetric and antisymmetric molecular orbitals reflect well the previous simple considerations on their origin. The homo ( $m$ ) is mainly localized on the sulfur atom, the atomic sulfur coefficient  $c_S$  being 0.65. This is in agreement with the experimental results relative to the donor character of the phenoxathiin derivatives [16] and the features of the respective cation-radicals [17] as well as with the previous PPP calculations [8,18]. The lomo ( $m + 1$ ) is an antisymmetric orbital localized on the benzenic rings. Taking into account the features of the phenoxathiin frontier

Table 5  
Photophysical parameters for **III** and **IV** in methanol; Stern–Volmer quenching by KI

Compound	$\tau_0$ (ns)	$\tau^a$ (ns)	$k_{f0} \times 10^{-7}(\text{s}^{-1})$	$k_f \times 10^{-7}(\text{s}^{-1})$	$k_{nr}^b \times 10^{-7}(\text{s}^{-1})$	$K_{sv}(\text{dm}^3 \text{mol}^{-1})$	$\tau^c$ (ns)	$k_f \times 10^{-7}(\text{s}^{-1})$	$k_{nr} \times 10^{-7}(\text{s}^{-1})$
<b>III</b>	31.8	2.6	3.1	38.5	35.4	45	4.1	24.4	21.3
<b>IV</b>	32.2	6.0	3.2	16.7	13.5	62	5.7	17.5	14.3

<sup>a</sup> Fluorescence lifetime calculated considering the relationship  $\Phi_f = \tau/\tau_0$ .

<sup>b</sup>  $k_f = k_{f0} + k_{nr}$ .

<sup>c</sup> Fluorescence lifetime calculated considering that the Stern–Volmer quenching is due to a diffusional controlled process with  $k_d = 10.87 \times 10^9 \text{ s}^{-1}$ .

Table 6  
Energies (eV) of the molecular orbitals implied in the emission properties

$\psi$	Symmetry	Benzene	I	II	III	IV
O(CO) lone pair	S		-11.42	-11.27	-11.60	-11.70
	A	-9.65	-10.23	-10.0	-10.86	-10.81
	A	-9.65	-10.18	-10.0	-10.43	-10.40
$m$	S		-9.31	9.28	-9.55	-9.48
	S		-7.80	-7.73	-8.08	-7.99
$m + 1$ (III, IV)	A				-0.87	-0.75
$m + 1$ (I,II); $m + 2$ (III, IV)	A	-0.25	-0.26	-0.25	-0.17	-0.31

orbitals it is expected that the  $m \rightarrow m + 1$  transition will imply a charge transfer from the sulfur atom toward both benzenic rings.

The same interaction schema is found for all the derivatives, the fluctuations in the energy values being within 0.6 eV. An overview of all the results in Table 6 points out that, for **I** and **II**, the molecular orbitals are quite similar, which is in agreement with the experimental results already discussed concerning the presence of the same excited state. The contours for the orbitals mainly implied in the emission properties are presented for **III** in Fig. 5.

In the case of the carbonyl-containing compounds, **III** and **IV**, besides the orbitals of phenoxathiin two new molecular orbitals are predicted:

- An orbital with energy ca. -10.81 eV in the range of the occupied molecular orbitals. Considering the coefficients of the atomic orbitals, this orbital was assigned to the carbonylic oxygen lone pair. A check of this assignment was made by comparing the energy and the expression of this orbital in a series of related carbonyl-containing compounds. The results in Table 7 point out that in all cases the energy of this orbital is similar, hence supporting the assignment made. The deep position of this orbital rules out the possibility that the first transition will have an  $n-\pi^*$  character.

- The most important difference between compounds **I**, **II** and **III**, **IV** lies in the presence, for the latter two, of a new low lying  $\pi^*$  orbital, intercalated between the

frontier orbitals of phenoxathiin and localized on the carbonyl group and the substituted benzene ring (especially on the carbon bonded to the sulfur atom). Therefore, the first excited state, corresponding to the  $m \rightarrow m + 1$  transition will have a different character for these compounds, and only the second transition,  $m \rightarrow m + 2$  will be similar to that of phenoxathiin.

The calculations explain the presence of the band at 300 nm in all the phenoxathiin derivatives and support the assumption of a different excited state for the carbonyl-containing compounds. However, as both transitions involve the highest occupied molecular orbital, it is expected that the resulted excited states will be characterized by a charge transfer from the sulfur atom.

The charge density distribution in the ground state points out a fairly similar value for the sulfur charge density for all the compounds,  $\Delta q_S \cong 0.48$ ; however, the dipole moments (Table 8) are low for **I** and **II** and high for **III** and **IV**; for the first compounds there is a symmetrical distribution over the whole molecule while for the other two the presence of the carbonyl group introduces some asymmetry in the charge density distribution.

The optimization of the first excited singlet and triplet states lead to the following results:

- A change of the molecular conformation; differing from the ground state, the phenoxathiin ring adopts a planar conformation. A slight distortion from the overall

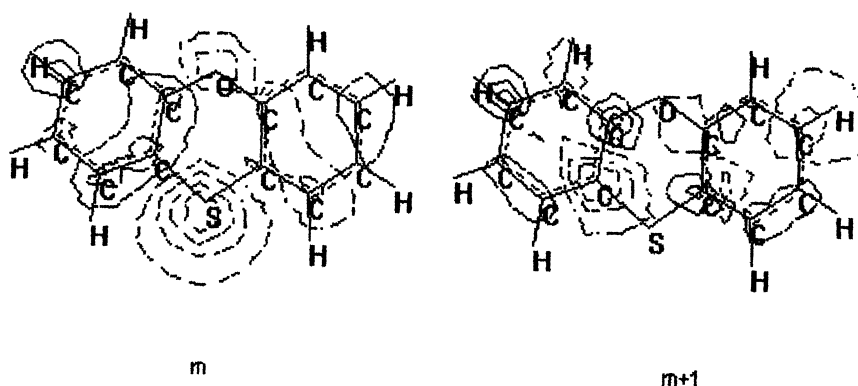


Fig. 4. Contours of the frontier molecular orbitals for phenoxathiin, **I**.

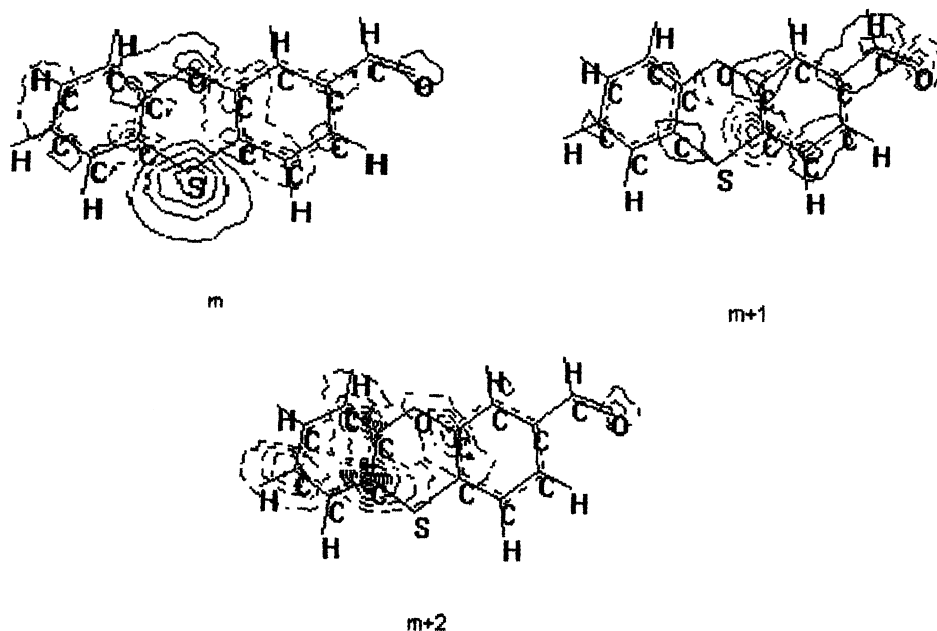


Fig. 5. Contours of the molecular orbitals,  $m$ ,  $m + 1$ ,  $m + 2$  for compound **III**.

Table 7  
Energy (eV) of the MO assigned to the carbonylic oxygen lone pair

CH <sub>2</sub> O	CH <sub>3</sub> CHO	<b>III</b>	<b>IV</b>	4-COCH <sub>3</sub> -diphenylsulfide	4-COCH <sub>3</sub> -diphenylether
-10.78	-10.72	-10.84	-10.80	-10.67	-10.69

planarity was noticed only for **IV**, the acetyl group being twisted by ca. 10° around the phenyl–acetyl bond;

– An increase in the dipole moments (Table 8) for all the compounds, in agreement with the charge transfer character of the first electronic transition, in spite of their different nature (the sulfur charge density,  $\Delta q_S \cong 0.89$  attest the transfer of almost one electron). Due to the asymmetric transfer already discussed, this effect is much enhanced for **III** and **IV**, thereby explaining the solvatochromicity experimentally observed. However, the theoretical values are lower than

those predicted by the Lippert–Mataga treatment, even for the lower acceptable values of the cavity radius. In order to improve the agreement, the optimization of the first singlet state ( $S_1$ ) for **III** were performed considering several levels of configurational interactions and the two possible planar conformers. The results are listed in Table 9. It can be remarked that although the heat of formation is not much modified, the excited dipole moment is more sensitive to the number and the types of mixed configurations. Larger dipole-moment values were determined by the inclusion in the C.I. calculations of all the excited states generated by the MO:  $m$ ,  $m + 1$ ,  $m + 2$ , as both  $m \rightarrow m + 1$  and  $m \rightarrow m + 2$  transitions lead, as already discussed, to charge transfer states. The C=O position does not bring about significant modifications in the dipole moment values, the maximum difference of ca. 0.5 D being obtained for **IVa** vs. **IVb**.

Table 8  
Singlet–triplet splitting ( $\text{cm}^{-1}$ ) and dipole moments (D) in the ground and excited singlet and triplet states calculated considering the configurational interaction between the states involving the frontier orbitals,  $m$ ,  $m + 1$

Compound	$\Delta E_{S-T}$	$\mu_{S0}$	$\mu_{S1}$	$\mu_{T1}$
<b>I</b>	4106	0.26	1.68	1.79
<b>II</b>	4099	0.40	1.75	1.86
<b>IIIa</b> <sup>a</sup>	5565	3.15	5.50	7.18
<b>IIIb</b> <sup>a</sup>	5737	3.30	5.20	7.40
<b>IVa</b> <sup>a</sup>	5288	3.09	5.23	6.97
<b>IVb</b> <sup>a</sup>	5572	3.33	4.70	7.00

<sup>a</sup> 'a' represents the conformer with the C=O group directed toward the heterocyclic oxygen and 'b' stands for the opposite in-plane conformer.

The calculated singlet–triplet splitting included also in Table 9 point out larger values for **III** and **IV** than for **I** and **II**. Assuming that the singlet–triplet gap may be a critical point in the nonradiative decays, we can expect a lower probability of intersystem crossing processes for the carbonyl containing compounds.

Table 9

Influence of the CI calculations on the excited-state heat of formation and dipole moment for **IV**

MO	$m \rightarrow m + 1$	$m - 1, m \rightarrow m + 1$	$m \rightarrow m + 1, m + 2$	$m - 2, m - 1, m \rightarrow m + 1$	$m - 1, m \rightarrow m + 1, m + 2$
$\Delta H(\text{kcal mol}^{-1})$	54.09	54.01	57.18	53.37	54.80
$\mu(\text{D})$	5.23	5.18	6.62	6.16	6.52

#### 4. Conclusions

The absorption and fluorescence data point out that the excited state properties of the phenoxathiin derivatives are deeply influenced by the type of the substituent. A significant increase in the emission quantum yields relative to the parent heterocycle is determined by the carbonyl-containing substituents, formyl and acetyl, whereas the methyl substitution does not perturb the electronic features of the phenoxathiin excited state. The strong dependence of the fluorescence maxima on the solvent polarity for **III** and **IV** attests a pronounced intramolecular charge transfer of the excited state (ICT state) and predicts an increase of the dipole moments of ca. 6–7 D. The behavior in protic solvents (alcohols) could not be rationalized in terms of the Lippert–Mataga treatment and some specific interactions, more likely of the hydrogen bond type can be assumed. Some experiments in protic solvents (methanol: water/1 : 9 v/v) on the inclusion complexes in  $\alpha$ - and  $\beta$ -cyclodextrines, which are now in progress at our laboratory, are expected to throw some light on these interactions.

The molecular orbital calculations support the experimental findings and explain the fluorescent properties of **III** and **IV** vs. **I** and **II** by a different excited state generated in the presence of a new vacant low-lying  $\pi^*$  orbital. It seems that a vacant orbital situated between the frontier molecular orbitals of phenoxathiin should be a prerequisite for improving the emission efficiency in the phenoxathiin class; other derivatives fulfilling this condition are now in study. The calculations also predict the intramolecular charge-transfer nature of the excited states, the donor center being the sulfur atom, even if the theoretical values for the dipole moments are lower than the experimental ones. It was found that, out of all the properties, the dipole moment is the most

influenced by the number and type of the excited states taken into account in the CI calculation of the first excited singlet.

#### References

- [1] M.B. Rijkov, V.A. Rodionov, A.N. Stepanov, *Z. Fiz. Him.* 63 (1989) 2515–2518.
- [2] William S. Jenks, Woojae Lee, David Shutter, *J. Phys. Chem.* 98 (1994) 2282–2289.
- [3] Charles B. Airaudo, A. Gayte-Sorbier, *Ann. Pharm. Fr.* 39 (1981) 359–368.
- [4] J. Karpinski, B. Starczewa, H. Puzanowska-Tarasiewicz, *Analy. Sci.* 12 (1996) 161–170.
- [5] Ovidiu Maior, Daniela Gavrilu, *Rev. Chim. (Buc)* 47 (1996) 127–133.
- [6] S.J. Strickler, R.A. Berg, *J. Chem. Phys.* 37 (1962) 814–822.
- [7] Mamoru Kamiya, *Bull. Chem. Soc. Jpn.* 45 (1972) 1589–1595.
- [8] Mihaela Hillebrand, V.Em. Sahini, *Rev. Roum. Chim.* 25 (1980) 625–631.
- [9] E. Lippert, *Z. Naturforsch.* 10a (1955) 541.
- [10] Saskia I. van Dijk, Piet G. Wiering, Cornelis P. Groen, Albert M. Brouwer, J. Verhoeven, *J. Chem. Soc. Faraday Trans.* 91 (1995) 2107–2114.
- [11] Wouter Verbouwe, Lucien Viaene, Mark Van der Auweraer, Frans C. De Schryver, H. Masuhara, R. Pansu, J. Faure, *J. Phys. Chem. A* 101 (1997) 8157–8165.
- [12] A. Vlahovici, A. Ofenberg, L. Cires, A. Pollet, A. Lablache-Combiere, *J. Luminiscence* 62 (1994) 227–236.
- [13] Rene Lapouyade, Alexander Kuhn, Jean-Francois Letard, Wolfgang Rettig, *Chem. Phys. Lett.* 208 (1993) 48–58.
- [14] H. Le Breton, B. Bennetau, Jean-Francois Letard, Rene Lapouyade, Wolfgang Rettig, *J. Photochem. Photobiol. A: Chem.* 95 (1996) 7–20.
- [15] Maria E. Amato, Antonio Grassi, Kurt J. Irgolic, Gikuseppe C. Pappalardo, Lajos Radics, *Organometallics* 12 (1993) 775–780.
- [16] Mihaela Hillebrand, O. Maior, V.Em. Sahini, *Rev. Roum. Chim.* 15 (1970) 149–152.
- [17] I. Baci, Mihaela Hillebrand, V.Em. Sahini, *J. Chem. Soc. Perkin Trans.* 2 (1974) 986–989.
- [18] Mihaela Hillebrand, V.Em. Sahini, *Rev. Roum. Chim.* 25 (1980) 631–634.